

Redox Switch-Off of the Ferromagnetic Coupling in a Mixed-Spin Tricobalt(II) Triple Mesocate

Marie-Claire Dul,[†] Emilio Pardo,^{*,†} Rodrigue Lescouëzec,[†] Lise-Marie Chamoreau,[†]
Françoise Villain,[†] Yves Journaux,^{*,†} Rafael Ruiz-García,^{‡,§} Joan Cano,^{*,‡,§} Miguel Julve,[‡]
Francesc Lloret,^{*,‡} Jorge Pasán,^{||} and Catalina Ruiz-Pérez^{||}

Institut Parisien de Chimie Moléculaire, Université Pierre et Marie Curie-Paris 6, UMR 7201, F-75252 Paris, France, Departament de Química Inorgànica, Institut de Ciència Molecular (ICMol) and Fundació General de la Universitat de València (FGUV), Universitat de València, E-46980 Paterna, Valencia, Spain, and Laboratorio de Rayos X y Materiales Moleculares, Departamento de Física Fundamental II, Universidad de La Laguna, E-38201 La Laguna, Tenerife, Spain

Received July 2, 2009; E-mail: emilio.pardo@uv.es; yves.journaux@upmc.fr; joan.cano@uv.es; francisco.lloret@uv.es

The design and synthesis of polytopic ligands that are able to self-assemble with transition-metal ions to form linear multiple-stranded helicates and related *meso*-helicates (so-called mesocates) with predictable electronic properties are major goals in metallo-supramolecular chemistry.^{1,2} Besides their interest as models for fundamental research on electron exchange (EE) and electron transfer (ET) phenomena between distant metal centers through extended bridges, this type of ligand-supported, linear polynuclear complex would also be of great importance in the “bottom-up” approach to molecular-level electronic devices.³

Our strategy in this field consists of using linear oligo-*m*-phenylene oxalamide (OPOXA) ligands that possess multiple oxamato and/or oxamidato donor groups separated by phenylene spacers with a meta substitution pattern (Figure 1a). Thus, the parent dicobalt(II) triple mesocate **1** with the ligand *N,N'*-1,3-phenylenebis(oxamate) (mpba) exhibits a weak ferromagnetic coupling ($J = +1.03 \text{ cm}^{-1}$) between the high-spin (HS) Co^{II} ($S = 3/2$) ions because of spin polarization effects across the triple *m*-phenylenediamidate bridge.⁴ As a natural extension of that work, we report here the synthesis and characterization by single-crystal X-ray diffraction (XRD) and X-ray absorption spectroscopy (XAS) of the longer tricobalt(II) triple mesocate analogue **2** with the new ligand oxamidate-*N,N'*-bis(3-phenyloxamate) (obmpox) and the corresponding tricobalt(II,III,II) monooxidized derivative **2^{ox}**. The magnetic properties of this unique **2/2^{ox}** redox couple indicate that oligo-*m*-phenylene oxalamide cobalt mesocates can behave as ferromagnetic “metal–organic switches” (MOSs) for the transmission of through-bond metal–metal EE interactions,⁵ by analogy with related molecular switches that are based on direct metal–metal ET interactions instead.⁶

Complexes **2** and **2^{ox}** were synthesized from the reaction of the diethyl ester acid derivative of the proligand $\text{H}_4\text{Et}_2\text{obmpox}$ with Co^{2+} nitrate (1:1 molar ratio) by using NaOH as the base in water under Ar and air atmospheres, respectively, and they were isolated as the sodium salts having formulas $\text{Na}_{12}[\text{Co}_3(\text{obmpox})_3] \cdot 33\text{H}_2\text{O}$ (**2**) and $\text{Na}_{11}[\text{Co}_3(\text{obmpox})_3] \cdot 30\text{H}_2\text{O}$ (**2^{ox}**). Complex **2** is slowly oxidized by atmospheric dioxygen in aqueous solution to give **2^{ox}** with ~45% transformation after 30 min (see the Supporting Information). Indeed, oxidation of **2** with H_2O_2 resulted in essentially quantitative formation of **2^{ox}** (>96%), whereas treatment of **2^{ox}** with hydrazine partially restored the original **2** in up to 78% yield.

Single-crystal XRD analysis of **2** confirmed the triple-stranded, *meso*-helicate-type structure of the linear tricobalt(II) anions,

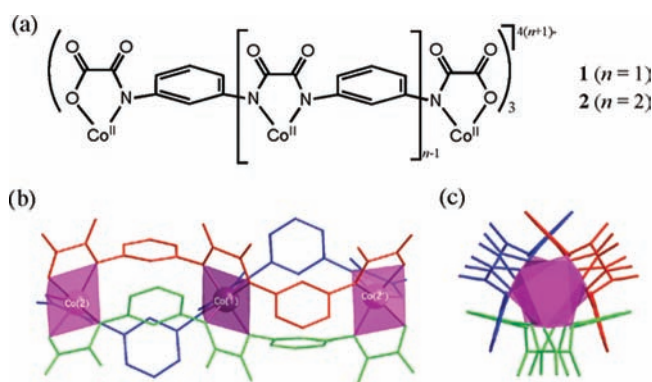


Figure 1. (a) Structure of the cobalt(II) triple mesocates with OPOXA ligands. (b) Front and (c) side views of the anionic tricobalt triple mesocate of **2**, showing each ligand strand and the metal coordination octahedra with Λ and Δ chiralities in different colors.

$[\text{Co}^{\text{II}}_3(\mu_3\text{-}\kappa^2\text{:}\kappa^2\text{-obmpox})_3]^{12-}$, with a crystallographically imposed D_3 molecular symmetry (Figure 1b). The side-by-side binding of the three nonplanar C_2 -symmetric tris(bidentate) obmpox⁶⁻ ligands around the three octahedral cobalt atoms affords a racemic mixture of heterochiral triple mesocates with alternating (Λ, Δ, Λ) and (Δ, Λ, Δ) chiralities (Figure 1c). This situation contrasts with the more common examples of homochiral [$(\Lambda, \Lambda, \Lambda)$ or (Δ, Δ, Δ)] triple helicates, which result instead from helical wrapping of the ligands around the metal centers.¹ The three collinear cobalt atoms of **2** are linked through a triple *m*-phenylenediamidate bridge. The intramolecular $\text{Co}(1) \cdots \text{Co}(2)$ and $\text{Co}(2) \cdots \text{Co}(2)$ distances are 6.8780(18) and 13.756(3) Å, respectively ($I = x - y, -y, 1/2 - z$).

The metal–ligand bond distances for the terminal cobalt atoms in **2** [$\text{Co}(2) - \text{N}(2) = 2.111(7)$ Å; $\text{Co}(2) - \text{O}(4) = 2.123(7)$ Å] are similar to those in **1** [$\text{Co} - \text{N} = 2.106(8)$ Å; $\text{Co} - \text{O} = 2.137(8)$ Å],⁴ in agreement with an HS d^7 Co^{II} ion in a trigonally distorted octahedral environment, CoN_3O_3 , formed by three amidate nitrogen and three carboxylate oxygen atoms from the bidentate oxamato groups [trigonal twist angle (θ) of $41.6(3)^\circ$]. However, the metal–ligand bond distances for the central cobalt atom of **2** are significantly shorter [$\text{Co}(1) - \text{N}(1) = 1.965(5)$ Å]. This agrees with a low-spin (LS) d^7 Co^{II} ion in an almost perfect octahedral environment, CoN_6 , formed by six amidate nitrogen atoms from the bidentate oxamidato groups [$\theta = 59.7(3)^\circ$]. Overall, this situation is as expected on the basis of the well-known stronger ligand field of the *N,N'*-oxamidato donor groups relative to the *N,O*-oxamato ones.⁷

The Co K-edge X-ray absorption near-edge structure (XANES) spectra of **2** and **2^{ox}** agree with mixed-spin, homovalent Co^{II} -

[†] Institut Parisien de Chimie Moléculaire, UMR 7201, Université Pierre et Marie Curie-Paris 6.

[‡] Departament de Química Inorgànica, ICMol, Universitat de València.

[§] FGUV, Universitat de València.

^{||} Departamento de Física Aplicada II, Universidad de La Laguna.

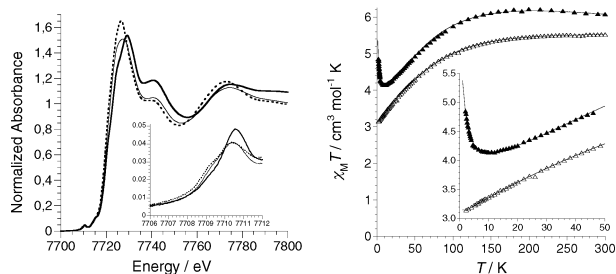


Figure 2. (a) Co K-edge XANES spectra of **2** (solid line) and **2^{ox}** (bold line) compared with that of **1** (dashed line). The inset shows the pre-edge region. (b) Temperature dependence of $\chi_M T$ for **2** (\blacktriangle) and **2^{ox}** (\triangle). The inset shows the low-temperature region (the solid lines are the best-fit curves).

(HS)Co^{II}(LS)Co^{II}(HS) and heterovalent Co^{II}(HS)Co^{III}(LS)Co^{II}(HS) formulations, respectively (Figure 2a). Notably, the asymmetry and broadness of the intense edge features corresponding to the 1s \rightarrow 4p transitions for **2** and **2^{ox}** in comparison with those of **1** indicate the coexistence of different spin and/or oxidation states for the terminal and central metal ions. Moreover, a shift to higher energy is observed for the main broad peak centered at 7729.0 eV in **2^{ox}** relative to the corresponding one centered at 7727.0 eV in **2**, which is in turn close in energy to the main sharp peak located at 7726.5 eV in **1**. This hypsochromic energy shift of 2.0 eV in **2^{ox}** results mainly from the increase in binding energy of the 1s core electrons as the oxidation state of the central metal ion increases. Thus, the main peak of the weak pre-edge features corresponding to the 1s \rightarrow 3d transitions appears similarly shifted at higher energy from 7710.4 eV in **1** and 2 to 7710.6 eV in **2^{ox}**. Similar oxidation-state-dependent edge and/or pre-edge shifts have been reported for other octahedral cobalt complexes.⁸

The plots of $\chi_M T$ versus T (where χ_M is the molar magnetic susceptibility per Co₃ unit and T the temperature) for **2** and **2^{ox}** are consistent with ferromagnetically coupled Co^{II}(HS)Co^{II}(LS)Co^{II}(HS) and uncoupled Co^{II}(HS)Co^{III}(LS)Co^{II}(HS) linear triads, respectively (Figure 2b). The increase in $\chi_M T$ for **2** in the low-temperature region is indicative of a weak ferromagnetic interaction between the two terminal HS Co^{II} ($S = 3/2$) ions and the central LS Co^{II} ($S = 1/2$) ion ($J = J_{12} = J_{12'} > 0$) (inset of Figure 2b). On the contrary, there is no sign of either ferro- or antiferromagnetic interaction between the two terminal HS Co^{II} ($S = 3/2$) ions ($J' = J_{22'} = 0$) across the central diamagnetic LS Co^{III} ($S = 0$) ion for **2^{ox}**, as expected given the large intramolecular metal–metal separation (~ 14 Å). The continuous decrease in $\chi_M T$ in the high-temperature region for both **2** and **2^{ox}** is attributed to spin–orbit coupling effects of the orbitally degenerate, terminal Co^{II} ions (4T_1) in a distorted octahedral geometry.⁹

The magnetic susceptibility data for **2** and **2^{ox}** were analyzed through the appropriate spin Hamiltonian for a linear trinuclear model (eq 1 with $S_2 = S_2' = 3/2$, $L_2 = L_2' = 1$, and $S_1 = 1/2$ and 0 for **2** and **2^{ox}**, respectively):

$$\begin{aligned} \hat{H} = & -J(\hat{S}_1 \cdot \hat{S}_2 + \hat{S}_1 \cdot \hat{S}_{2'}) - J'(\hat{S}_2 \cdot \hat{S}_{2'}) + \\ & \alpha\lambda(\hat{L}_2 \cdot \hat{S}_2 + \hat{L}_{2'} \cdot \hat{S}_{2'}) \\ & + \Delta(\hat{L}_{2z}^2 + \hat{L}_{2'z}^2) + g_1\hat{S}_{1z}\beta H + g_2(\hat{S}_{2z} + \hat{S}_{2'z})\beta H + \\ & \alpha(\hat{L}_{2z} + \hat{L}_{2'z})\beta H \end{aligned} \quad (1)$$

where g_1 and g_2 ($=g_e$) are the Zeeman factors, λ is the spin–orbit coupling parameter, Δ is the axial orbital splitting parameter, and α is an orbital reduction parameter.⁹ A good fit of the experimental data was obtained (for $J' = 0$ cm⁻¹) with $J = +1.2$ cm⁻¹, $g_1 = 2.20$, $\lambda = -130$ cm⁻¹, $\Delta = 120$ cm⁻¹, and $\alpha = 1.10$ for **2** and $\lambda = -109$ cm⁻¹, $\Delta = 239$ cm⁻¹, and $\alpha = 1.10$ for **2^{ox}**. The axial orbital splitting of the terminal HS Co^{II} ions for **2^{ox}** is greater than that for **2**, likely reflecting a larger distortion of the octahedral geometry. The weak but nonnegligible ferromagnetic coupling between the central LS Co^{II} ion and the terminal HS Co^{II} ions for **2**, in spite of the moderately large intramolecular metal–metal separation (~ 7 Å), suggests that the exchange interaction involves a spin polarization mechanism through the *m*-phenylene spacers, as in **1** ($J = +1.0$ cm⁻¹).⁴

In conclusion, the heterotropic nature of the tailored ligand obmpox⁶⁻ allows for the side-by-side self-assembly of Co²⁺ ions to afford two unique examples of homo- and heterovalent mixed-spin trinuclear triple mesocates under either anaerobic and aerobic conditions, respectively. The spins of the metal centers are ferromagnetically coupled in the homovalent tricobalt(II) mesocate (“ON” state), whereas they are uncoupled in the heterovalent tricobalt(II,III,II) mesocate (“OFF” state). Current efforts are devoted to the synthesis of other examples of oligo-*m*-phenylene oxalamide mesocates as potential candidates for electrically triggered magnetic molecular switches.

Acknowledgment. This work was supported by the Ministerio de Educación y Ciencia (MEC, Spain) (Projects CTQ2007-61690, CSD2007-00010, and MAT2007-60660), the Generalitat Valenciana (GV, Spain) (Project PROMETEO/2009/108), and the Ministère de l’Enseignement Supérieur et de la Recherche (MESR, France). E.P. and M.-C.D. thank the MEC and MESR for grants.

Supporting Information Available: Preparation and physical characterization data of the ligand and complexes **2** and **2^{ox}**, electronic spectroscopic studies with oxidants and reductants, and a CIF file for **2**. This material is available free of charge via the Internet at <http://pubs.acs.org>.

References

- Piguet, C.; Bernardinelli, G.; Hopfgartner, G. *Chem. Rev.* **1997**, *97*, 2005.
- (a) El-Ghayoury, A.; Harriman, A.; De Cian, A.; Fischer, J.; Ziessel, R. *J. Am. Chem. Soc.* **1998**, *120*, 9973. (b) Aromí, G.; Berzal, P. C.; Gamez, P.; Roubeau, O.; Kooijman, H.; Spek, A. L.; Driessen, W. L.; Reedijk, J. *Angew. Chem., Int. Ed.* **2001**, *40*, 3444.
- Bera, J. K.; Dunbar, K. R. *Angew. Chem., Int. Ed.* **2002**, *41*, 4453.
- Cangussu, D.; Pardo, E.; Dul, M.-C.; Lescouëzec, R.; Herson, P.; Journaux, Y.; Pedroso, E. F.; Pereira, C. L. M.; Muñoz, M. C.; Ruiz-García, R.; Cano, J.; Amorós, P.; Julve, M.; Lloret, F. *Angew. Chem., Int. Ed.* **2008**, *47*, 4211.
- (a) Shultz, D. A.; Kumar, R. K. *J. Am. Chem. Soc.* **2001**, *123*, 6431. (b) Shores, M. P.; Long, J. R. *J. Am. Chem. Soc.* **2002**, *124*, 3512.
- (a) Berry, J. F.; Cotton, F. A.; Daniels, L. M.; Murillo, C. A. *J. Am. Chem. Soc.* **2002**, *124*, 3212. (b) Lin, S. Y.; Chen, I. W. P.; Chen, C. H.; Hsieh, M. H.; Yeh, C. Y.; Lin, T. W.; Chen, Y. H.; Peng, S. M. *J. Phys. Chem. B* **2004**, *108*, 959.
- Ruiz, R.; Surville-Barland, C.; Aukauloo, A.; Anxolabèhere-Mallart, E.; Journaux, Y.; Cano, J.; Muñoz, M. C. *Dalton Trans.* **1997**, 745.
- Roux, C.; Adams, D. M.; Itié, J. P.; Polian, A.; Hendrickson, D. N.; Verdager, M. *Inorg. Chem.* **1996**, *35*, 2846.
- Lloret, F.; Julve, M.; Cano, J.; Ruiz-García, R.; Pardo, E. *Inorg. Chim. Acta* **2008**, *361*, 3432.

JA9052202